Open Research Online

The Open University's repository of research publications
and other research outputs

Infrared spectroscopic characterization of organic matter associated with microbial bioalteration textures in basaltic glass

Journal Item

For guidance on citations see FAQs.

Version: Version of Record

Link(s) to article on publisher's website:
http://dx.doi.org/doi:10.1089/ast.2010.0604

oro.open.ac.uk

Infrared Spectroscopic Characterization of Organic Matter Associated with Microbial Bioalteration Textures in Basaltic Glass

L.J. Preston,[1] M.R.M. Izawa,[2] and N.R. Banerjee[2]

Abstract

Microorganisms have been found to etch volcanic glass within volcaniclastic deposits from the Ontong Java Plateau, creating micron-sized tunnels and pits. The fossil record of such bioalteration textures is interpreted to extend back ∼3.5 billion years to include meta-volcanic glass from ophiolites and Precambrian greenstone belts. Bioalteration features within glass clasts from Leg 192 of the Ocean Drilling Program were investigated through optical microscopy and Fourier transform infrared (FTIR) spectroscopy of petrographic thin sections. Extended depth of focus optical microscopic imaging was used to identify bioalteration tubules within the samples and later combined with FTIR spectroscopy to study the organic molecules present within tubule clusters. The tubule-rich areas are characterized by absorption bands indicative of aliphatic hydrocarbons, amides, esters, and carboxylic groups. FTIR analysis of the tubule-free areas in the cores of glass clasts indicated that they were free of organics. This study further constrains the nature of the carbon compounds preserved within the tubules and supports previous studies that suggest the tubules formed through microbial activity. Key Words: Infrared— Organics—Bioalteration—Basalt glass. Astrobiology 11, 585–599.

1. Introduction

STUDIES HAVE SHOWN that microbes play an important role in the weathering of basaltic glasses in the terrestrial environment (*e.g.,* Thorseth *et al.,* 1992, 1995, 2003; Fisk *et al.,* 1998; Torsvik *et al.,* 1998; Furnes *et al.,* 2001a, 2001b, 2008; Staudigel *et al.,* 2006, 2008a, 2008b; Banerjee *et al.,* 2008) and that basaltic glass may act as a growth medium for a variety of microbes, in that it provides a source of energy and nutrients (*e.g.,* Banerjee and Muehlenbachs, 2003; Staudigel *et al.,* 2006, 2008b). Biological communities are inferred to create characteristic bioalteration textures (Fisk *et al.,* 1998; Furnes *et al.,* 2001a) (Fig. 1a) within volcanic glasses found associated with ocean basins, ophiolites, and greenstone belts. These textures are located predominantly in the upper 300 m of the oceanic crust and are observed throughout the geological record, dating back ∼3.5 Ga (Furnes and Muehlenbachs, 2003; Furnes *et al.,* 2004, 2008; Banerjee *et al.,* 2006, 2007, 2008; Peckmann *et al.,* 2008; Staudigel *et al.,* 2008b).

Bioalteration textures within basaltic glasses have been observed to be associated with enrichments of carbon and other biologically important light elements (*e.g.,* Banerjee and Muehlenbachs, 2003). The origin of these elements has been extensively investigated to infer a biotic or abiotic origin. Electron probe microanalysis detected carbon, potentially present in an organic form. This is implied, as the carbon was not associated with cations such as Ca, Mg, or Fe, which may indicate a carbonate source if present (Banerjee and Muehlenbachs, 2003). Tubular bioalteration structures in Ontong Java Plateau (OJP) glass shards that were stained with ethidium bromide revealed the probable presence of nucleic acids (Banerjee and Muehlenbachs, 2003). Organic carbon associated with tubular bioalteration was also detected by Benzerara *et al.* (2007) via synchrotron transmission X-ray microscopy. These bioalteration textures and associated geochemical features have been used as a signature of former microbial activity.

The nature of the organic compounds associated with bioalteration textures in basaltic glass, however, has not yet been fully characterized. In the present study, attenuated total reflectance (ATR) Fourier transform infrared (FTIR) spectroscopy was employed to further elucidate the nature of carbon found to be associated with bioalteration textures within samples of volcaniclastic tuff from the OJP, which was previously studied by Banerjee and Muehlenbachs (2003) and Izawa et al (2010a).

---

[1]Centre for Planetary Science and Exploration (CPSX) and [2]Department of Earth Sciences, The University of Western Ontario, London, Ontario, Canada.
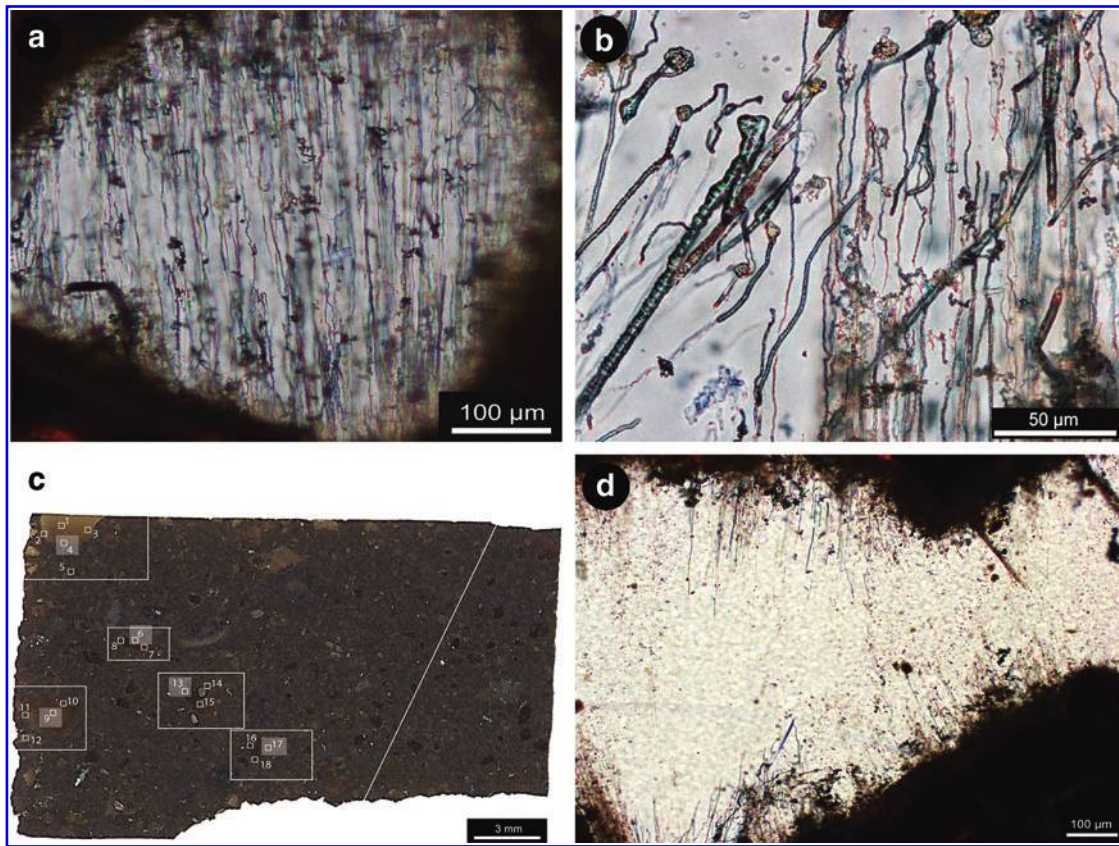
FIG. 1. (**a**) Transmitted light image of a glass fragment of this study crosscut by tubule structures. (**b**) A magnified view of the different tubule textures observed within glass clasts. (**c**) Thin section map of sample 1184A 13R3 145-148A with sampling sites and clasts numbered and shown in boxes, respectively. Areas shaded denote spot localities of analyses described in the text. (**d**) A transmitted light image of the glass clast where analyses 16, 17, and 18 were taken. Dense clusters of tubules are seen radiating from the glass edges toward the tubule-free core. Color images available online at www.liebertonline.com/ast

2. Geological Setting and Sampling

The OJP is the world's largest volcanic oceanic plateau and covers >1.6 million km^2 with a crustal volume of 40–50 million km^3 (Mahoney, 1987; Coffin and Eldholm, 1993). The rock samples for this study included fine to coarse-grained volcaniclastic rocks with tuff, lapilli tuff, and lapillistone. For a detailed description of all units recovered see Mahoney *et al.* (2001). The volcaniclastic rocks of interest consist of ash- to lapilli-sized lithic clasts and vitric shards; accretionary lapilli; armored lapilli; and crystal fragments set in a matrix of fine-grained vitric and lithic ash, clay, and other alteration minerals cemented by smectite, analcime, calcite, rare celadonite, and several zeolites (Mahoney *et al.*, 2001; Banerjee *et al.*, 2004). Vitric clasts, either completely altered to clay or variably altered with fresh glass cores, were studied with the intent to observe microbial alteration textures in volcanic glasses (Fig. 1a) (*e.g.*, Banerjee and Muehlenbachs, 2003). These samples contain some of the best-preserved, highly diverse, and abundant evidence of microbial alteration of volcanic glasses (Fig. 1b). Two distinct types of microbial alteration were observed as endolithic microborings in the basaltic glass, termed tubular and granular textures. Tubular textures (Fig. 1a, 1b) are the subject of this study. They are more easily recognized, albeit less common, as they are distinctive and larger, typically a few microns in diameter

and up to hundreds of microns in length (Banerjee and Muehlenbachs, 2003).

In both tubular and granular textures, it is inferred that microbes colonize exterior surfaces or surfaces of cracks and begin to dissolve the rock through changes in pH at their contact area (*e.g.*, Thorseth *et al.*, 1995; Torsvik *et al.*, 1998; Furnes *et al.*, 2001a, 2001b; Banerjee and Muehlenbachs, 2003; Staudigel *et al.*, 2006, 2008a, 2008b). Bioalteration textures are initially hollow but may be filled and preserved by a variety of authigenic mineral phases, including phyllosilicates, zeolites, Fe-oxyhydroxides, and titanite (Banerjee and Muehlenbachs, 2003; Staudigel *et al.*, 2006; Benzerara *et al.*, 2007). Early mineralization of bioalteration textures with minerals, such as titanite, enables their preservation for geologically long periods of time (*e.g.*, Furnes *et al.*, 2004; Banerjee *et al.*, 2007, 2008; Staudigel *et al.*, 2008a; Izawa *et al.*, 2010a, 2010b). Titanite (CaTiSiO$_5$) is a particularly important mineral that contributes to preservation of traces of microbial activity in basaltic glass (*e.g.*, Furnes *et al.*, 2004; Banerjee *et al.*, 2006, 2007, 2008), as it can enable the preservation of morphological and chemical signatures of biological activity, either within the titanite itself or by preserving biologically important elements at grain boundaries (Furnes *et al.*, 2004; Banerjee *et al.*, 2006, 2007, 2008). Observation of cross-cutting relationships (*e.g.*, Furnes *et al.*, 2004), *in situ* detection of titanite in seafloor basaltic glasses (Izawa *et al.*, 2010b), and

direct dating of titanite in tubular bioalteration textures from metamorphosed basaltic glasses (Banerjee *et al.*, 2007) have all indicated that tubule formation begins soon after basaltic glass emplacement and tubule formation and mineralization occur penecontemporaneously.

The samples for this study were recovered during Leg 192 of the Ocean Drilling Program (ODP) from Hole 1184A on the eastern lobe of the OJP at a water depth of 1661.1 m. Thin section 1184A 13R3 145-148A of glass-rich volcaniclastic core was used for the bulk of this study (Fig. 1c) to identify biomolecules within areas that host abundant tubular bioalteration textures (Fig. 1d). Reflectance FTIR spectroscopy was used, as characteristic fundamental vibrational modes that correspond to molecular bonds in organic molecules can be detected and characterized in the mid-IR region, 4000–700 cm^{-1} (2.5–14.2 μm).

3. Methods

3.1. Contamination

Contamination is an issue that strikes almost every form of life-detection research. Further, the issue of contamination leads inevitably to a fundamental philosophical problem: it is impossible to prove non-existence. It is possible, however, to exclude many potential sources of contamination and thus greatly reduce the probability that contamination exists. To this end, we prepared the thin sections studied by using alumina polishing compounds and non-organic lubricants for polishing. The section was kept in a sealed container and handled minimally and only with sterile nitrile gloves. The section was Ar sputtered to remove surface contamination prior to analysis.

3.2. Optical petrography

The OJP thin section was polished to produce a 30 μm thick section with a smooth surface for both optical imaging and reflectance FTIR measurements. This section contained >20 glass shards of various sizes, containing abundant tubules (Fig. 1d). The bulk of the sample is fine-grained and nearly opaque, which rendered transmitted light ineffective for imaging; however, this was not the case for the glass shards and tubules. These were imaged in plane-polarized light with a Nikon Eclipse LV100 POL petrographic microscope equipped with a Nikon DS-Ri1 12 Mpixel camera. Images of tubule-rich glass were acquired at ~0.4 μm spacing in the *z* direction, with the in-focus areas merged to create an extended depth of focus image stack of 30–40 images. This was accomplished by using Nikon Elements software.

3.3. Infrared and Fourier transform infrared spectroscopy

Infrared spectroscopy is based on the absorption of polychromatic electromagnetic radiation by matter due to the different vibrational modes of chemical bonds within a substrate. For a molecule to show IR absorptions, that is, to be "infrared-active," an electric dipole moment of the molecule must change during the vibration. The larger the dipole moment change, the more intense the absorption band observed. An IR spectrum is commonly obtained by passing IR radiation through, or reflecting it from, a sample and deter-

mining what fraction of the incident radiation is absorbed at each particular energy. The energy at which any peak in an absorption spectrum appears corresponds to the frequency of the vibration of part of a molecule, which is diagnostic for various functional groups within molecules. For a detailed description of IR spectroscopy, molecular symmetry, and group theory, see books by Diem (1993), Günzler and Gremlich (2002), and Stuart (2004).

Fourier transform infrared spectroscopy is based on the idea that interference of radiation between two beams yields an interferogram. The basic principles and advantages of modern FTIR spectroscopy were explained in detail by Diem (1993) and Griffiths and de Haseth (1986). Various FTIR measurement techniques can be used; however, ATR is the technique used here. In FTIR-ATR spectroscopy, the IR beam is reflected within an IR-transparent internal reflection element. An evanescent wave of the same frequency as the incoming IR light penetrates through the interface into the optically thinner medium, such as a thin section, that is adjacent to the interface. A sample spectrum is therefore obtained from a thin layer adjacent to the crystal surface, with the depth of penetration limited to a fraction of the wavelength (Harrick, 1967; Goos and Hähnchen, 1964). Most sample preparation methods for FTIR spectroscopy can be destructive; however, the ATR tool enables analyses to be conducted directly at specific sites of interest within a thin section, which preserves sample integrity such that the sample can be used in other studies.

Over the last 50 years, IR spectroscopy has been successfully applied to the characterization of chemical compounds within materials. More recently, transmission IR microspectroscopy has been employed for characterizing individual microscopic components of sedimentary organic matter (Thiessen, 1925; Brenner, 1984; Blob *et al.*, 1987; Landais and Rochdi, 1990; Rochdi and Landais, 1991). So far, most applications of IR and micro-IR techniques have been concentrated on the relative abundance of aliphatic C–H, aromatic C=C, and acid C=O bands. The functional groups of peptide and protein structures, polysaccharides, phospholipids, and nucleic acids can be observed and yield a spectrum with a high content of information. The aliphatic stretching region in particular will be described in this study, which was first unraveled by Painter *et al.* (1981) on the IR study of coal. The authors identified five bands in the stretching vibration region between 3000 and 2800 cm^{-1}, which correspond to the CH$_3$ asymmetrical stretching vibration at 2956 cm^{-1}, the CH$_2$ asymmetrical stretching vibration at 2923 cm^{-1}, the C–H stretching vibration at 2891 cm^{-1}, the CH$_3$ symmetrical stretching vibration at 2864 cm^{-1}, and the CH$_2$ symmetrical stretching vibration at 2849 cm^{-1}. There can be slight deviations from these values by up to 8 cm^{-1}, depending upon the resolution of the instrument being used. This study is also interested in the minerals found in association with the bioalteration structures. The "fingerprint region" of the mid-IR (between 500 and 1200 cm^{-1}) allows for the observation of not only organics as described above but also the absorption bands of minerals created by vibrations within a crystal lattice.

Fourier transform infrared–attenuated total reflectance spectroscopy was carried out on all samples by using a Bruker IFS55 FTIR with a Baseline Horizontal ATR attachment equipped with a germanium crystal, under an IRScope

II microscope. The IR microscope is a sampling accessory used to obtain IR spectra of very small samples. The microscope provided visual assessment of the sample and condensed the IR beam for spectral acquisition. Analyses of polished thin sections were carried out at Surface Science Western at a spectral resolution of $4\,cm^{-1}$, with a scan and sample background of 100 scans, over a spectral range of $4000–700\,cm^{-1}$ ($2.5–14.2\,\mu m$); analysis focused on a spot size between 50 and $60\,\mu m$ in diameter. All analyses were calibrated to the ATR-equipped germanium crystal, and atmospheric H_2O and CO_2 bands were subtracted out. Measurements were carried out on the pure glass thin sections surrounding the samples and the mounting media to identify contaminants and enable the removal of these contaminants from the spectra obtained. However, these media did not impact the analyses in this study. To calculate the integrated band intensities for component bands in the C–H stretching vibrational frequency region mentioned earlier, Fourier self-deconvolution is required to determine the center frequencies of the C–H moieties. A curve-fitting routine was then employed to expand the region. The curve-fitting procedure within the OPUS program was used, based on the damped least-squares optimization algorithm developed by Levenberg and Marquardt (Levenberg, 1944; Marquardt, 1963). The band shape used in the curve-fitting procedure was a linear combination of 100% Lorentzian+Gaussian bands. The residual RMS error was below 10^{-3} for all fitted data.

To enable ease of understanding of the spectra to follow, refer to Table 1 for a list of the characteristic absorption bands and vibrational modes of the inorganic and organic molecules identified in this study. Spectral bands are assigned with reference to the literature.

4. Results

Fourier transform infrared–attenuated total reflectance spectroscopic measurements of three representative tubule-rich areas within a number of glass shards are described. Areas observed to be highly distinct from one another were sampled within the glass shards but were found to yield very similar spectra. Measurements were also taken of areas with no observable tubules for comparison. The mid-IR spectrum between 4000 and $500\,cm^{-1}$ can display characteristic bands of minerals and organic functional groups suitable for the characterization of microorganisms and their constituent molecules. The tubules analyzed in this study are not wide enough to fill the entire measurement area; consequently, there is a strong contribution to the FTIR spectra from the glass and minerals present.

4.1. Tubule-rich areas

Analyses were first directed at Spot 4 (Fig. 1c), which is located at the edge of a large glass shard (Fig. 2a) and was observed to contain abundant tubules extending from the rim into the clast (Fig. 2b).

Mineralogy. The FTIR absorption bands displayed in Fig. 2c were obtained at the site shown in Fig. 2b. Bands at 981 and $723\,cm^{-1}$ are the Si–O asymmetric stretching vibrational mode of SiO_4 tetrahedra, and Si–O or Si–O–Al

TABLE 1. ORGANIC AND MINERALOGICAL FTIR ABSORPTION BAND FREQUENCIES FROM THIS STUDY ARE SHOWN, INCLUDING ASSIGNMENTS AND POTENTIAL ORIGINS

Wavenumber (cm^{-1})	Assignment	Potential Origin
Mineralogy		
3569–3581*	OH symmetric stretch	Water molecules
3401–3403*	OH asymmetric stretch	Water molecules
3270–3272*	OH asymmetric stretch	Water molecules
900–1100♦×	Si–O asymmetric stretch	SiO$_4$ tetrahedra, glass
720–740♦×	Si–O, Si–O–A1 symmetric bend, Ti–O stretch	SiO$_4$ tetrahedra, glass or TiO$_6$ octahedra
678–692×	Ti–O stretch	TiO$_6$ octahedra
Organics♣		
2956	CH$_3$ asymmetrical stretch	Lipids
2920	CH$_2$ asymmetrical stretch	Lipids
2870	CH$_3$ symmetrical stretch	Lipids
2850	CH$_2$ symmetrical stretch	Lipids
1743	C=O stretch	Ester, fatty acids
1653	Amide I (80% C=O stretch; 10% C–N stretch; 10% N–H bend)	Proteins
1567–1548	Amide II (60% N–H bend; 40% C–N stretch)	Proteins
1470	CH$_3$ asymmetrical bend/CH$_2$ scissoring	Lipids
1468	CH$_2$ scissoring	Lipids
1460	CH$_3$ asymmetrical bend	Lipids
1430	C–O–H in-plane bending	Carboxylic group
1401	N$^+$ (CH$_3$)$_3$ symmetrical bend	Lipids
1320	C–O stretch	Carboxylic group
1299	Amide III (30% C–N stretch; 30% N–H bend; 10% C=O stretch; 10% O=C–N bend; 20% other)	Proteins

Organic bands (indicated by ♣) compiled from Stuart and Ando (1997), Stuart (2004), Tamm and Tatulian (1997), Krimm and Bandekar (1986), Jackson and Mantsch (1995), Arrondo *et al.* (1993), Schmitt and Flemming (1998). Mineralogy band positions: ♦Dufresne *et al.* (2009); ×Zhang *et al.* (2002) and *Verma *et al.* (2007).
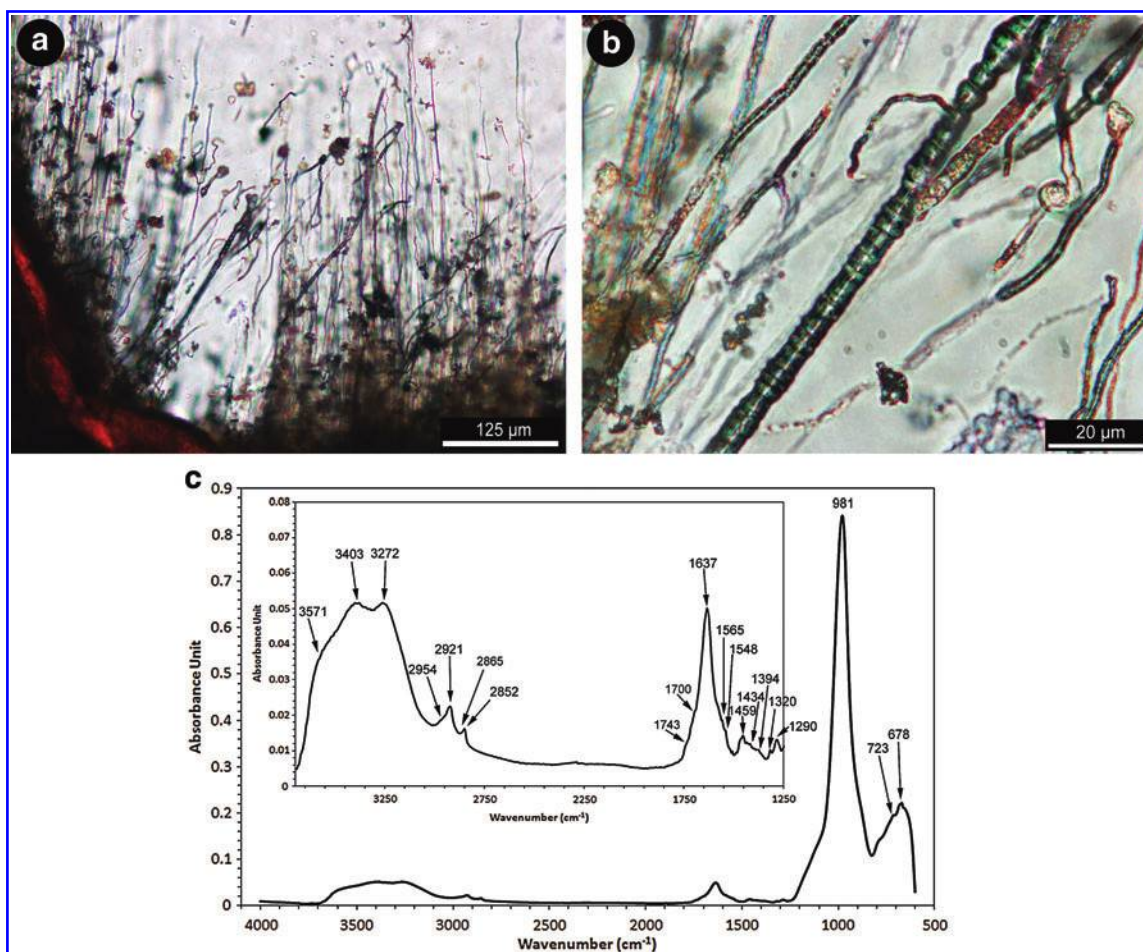
FIG. 2. Transmitted light images and FTIR absorbance spectra from Spot 4. (**a**) Overview of Spot 4. Tubule clusters are visible radiating from the palagonite-rich clast rim. (**b**) Extended depth of field view of the area analyzed by FTIR spectroscopy to create the spectrum in (c). The large tubule in the center of the image resembles that of the annulated ichnofossil *Tubulohyalichnus annularis* isp. nov. of McLoughlin *et al.* (2009). Simple unornamented and unbranched *Tubulohyalichnus simplus* isp. nov. (McLoughlin *et al.,* 2009) are also visible crosscutting the image, with one apparently branching off from the central *Tubulohyalichnus annularis* isp. nov. tubule. (**c**) An FTIR spectrum from Spot 4 showing Si–O and Ti–O stretching absorption bands. Inset shows an expanded absorbance spectrum, at the expense of the silicate glass, to identify the band positions of the main organic functional groups detected. Band frequencies match those described within the text and in Table 1. Color images available online at www.liebertonline.com/ast

symmetric bending vibrational mode, respectively. The $723 \, cm^{-1}$ band can also be derived as a Ti–O stretching vibrational mode of TiO_6 octahedra (Table 1), as can the absorption band observed at $678 \, cm^{-1}$. Absorption bands at 3571, 3403, and $3272 \, cm^{-1}$ in the Fig. 2c inset are assigned to the OH symmetric stretching vibrational mode of partially hydrogen-bonded water molecules, and the asymmetric and symmetric OH stretch of water molecules fully hydrogen-bonded with surrounding water molecules, respectively (Verma *et al.,* 2007). This region of OH bands can be contributed through Si–OH stretching vibrational modes relating to the silicate minerals present, or are hydrogen-bonded to an organic matrix.

Organics. Fourier transform infrared absorption bands of aliphatic C–H moieties can be seen at 2954, 2921, 2865, and $2852 \, cm^{-1}$ (Fig. 2c inset). The shoulder band absorption at $2954 \, cm^{-1}$ and the absorption band at $2921 \, cm^{-1}$ are derived from the asymmetric stretching vibrational modes of CH_3

and CH_2, respectively. A weak absorption band at $2865 \, cm^{-1}$ relates to the symmetric stretching vibrational mode of CH_3, while the symmetric CH_2 stretching vibrational mode appears at $2852 \, cm^{-1}$ (see Table 1 and references therein). An absorption band at $1637 \, cm^{-1}$ may be derived from the Amide I C=O stretching vibrational mode (Krimm and Bandekar, 1986). This absorption band frequency, however, overlaps the H_2O bending vibrational mode. Shoulder absorption bands appear on the Amide I/H_2O band at 1743 and $1700 \, cm^{-1}$, due to C=O stretching vibrational modes (Schmitt and Flemming, 1998, and references therein), and at 1565 and $1548 \, cm^{-1}$, corresponding to Amide II vibrational modes (Krimm and Bandekar, 1986). The absorption band at $1290 \, cm^{-1}$ matches that of the Amide III vibrational mode (Krimm and Bandekar, 1986). An asymmetric bending vibrational mode of aliphatic CH_3 is seen at $1459 \, cm^{-1}$ (*e.g.,* Tamm and Tatulian, 1997). Absorption bands at 1434, 1394, and $1320 \, cm^{-1}$ can be identified as C–O–H, CO_2, and C–O vibrational modes.

Analyses were also directed at Spot 6 (Fig. 1c), which is located along the palagonite-rich edge of a tubule-rich glass clast (Fig. 3a). An image of one of the tubule-rich areas analyzed is shown in Fig. 3b.

Mineralogy. An FTIR absorption band occurs at $981\,cm^{-1}$ that is assigned to the asymmetric stretching vibrational mode of Si–O bonds in SiO_4 tetrahedra (Fig. 3c). An absorption band at $740\,cm^{-1}$ is a Si–O, Si–O–Al symmetric bending vibrational mode or a Ti–O stretching vibrational mode. A Ti–O stretching vibrational mode of TiO_6 octahedra is located at $692\,cm^{-1}$ (see Table 1 and references therein). Absorption bands at 3581, 3384, and $3270\,cm^{-1}$ are assigned to the symmetric OH stretching vibrational mode of partially hydrogen-bonded water molecules, and asymmetric and symmetric OH stretching vibrational modes of water molecules that are fully hydrogen-bonded with surrounding water molecules, respectively (Fig. 3c inset). The OH ab-

sorption bands are contributed through Si–OH stretching vibrational modes or those that are hydrogen-bonded to an organic matrix (Verma *et al.*, 2007).

Organics. Fourier transform infrared absorption bands attributed to organics within the tubule-rich areas are shown in the inset of Fig. 3c. The aliphatic C–H moiety absorption bands appear at 2954, 2921, 2869, and $2850\,cm^{-1}$, corresponding to the asymmetric stretching vibrational modes of CH_3 and CH_2, and the symmetric stretching vibrational modes of CH_3 and CH_2, respectively. An absorption band at $1643\,cm^{-1}$ may be derived from the Amide I C=O stretching vibrational mode. This same band, however, can be attributed to the H_2O bending mode. Shoulder absorptions appear on the Amide I/H_2O band at 1743, 1602, and $1567\,cm^{-1}$. The bands at 1743 and $1602\,cm^{-1}$ are attributed to the C=O stretching vibrational mode and to either the C–C or asymmetric C=N vibrational modes, respectively, while the
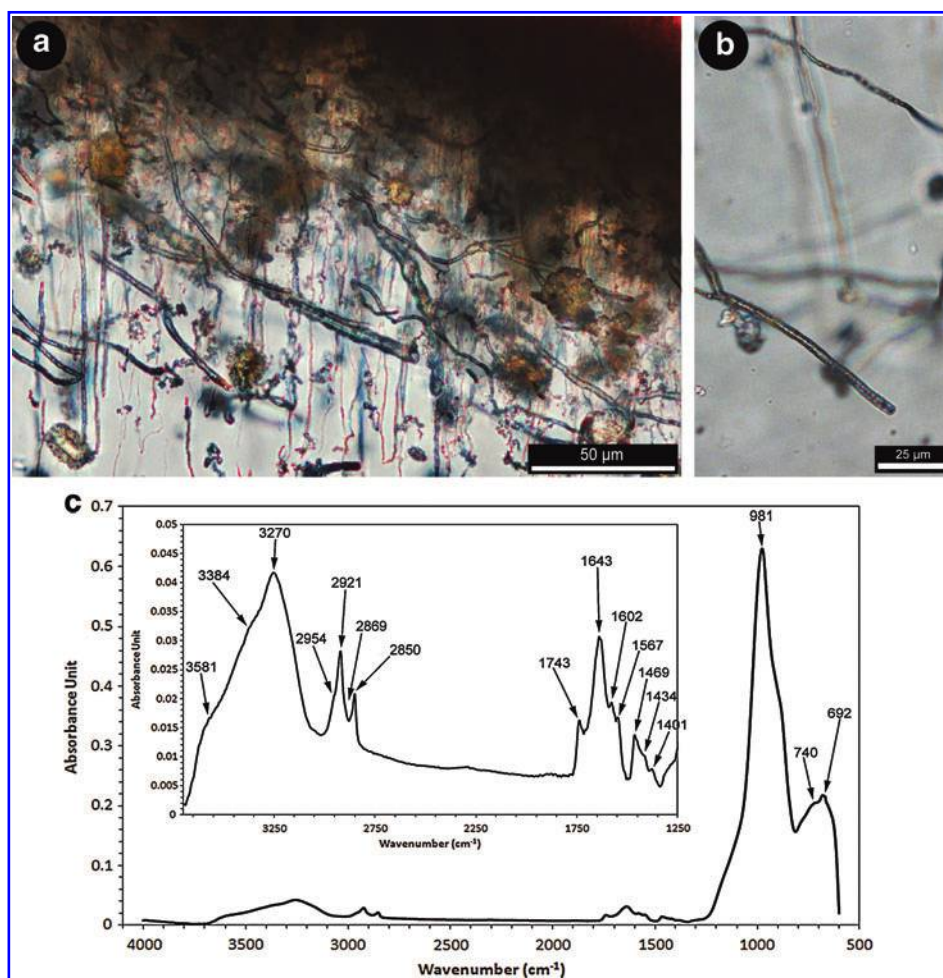
FIG. 3. Transmitted light images and FTIR absorbance spectra from Spot 6. (**a**) Extended depth of field image of the area analyzed around Spot 6 with numerous filaments of both *Tubulohyalichnus annularis* isp. nov. and *Tubulohyalichnus simplus* isp. nov. observed either free within the glass matrix or surrounded by palagonite. It is observed that many of the *Tubulohyalichnus simplus* isp. nov. are extending perpendicular to the clast edge, whereas the *Tubulohyalichnus annularis* isp. nov. are almost running parallel to the clast rim. (**b**) Magnified transmitted light image of an individual *Tubulohyalichnus simplus* isp. nov. tubule, showing no evidence of mineralization. (**c**) FTIR spectrum of Spot 6. Si–O and Ti–O stretching absorption bands are observed with the inset highlighting the main organic vibrational modes of aliphatic hydrocarbons, esters, amides, and carboxylic acids at the expense of the silicate glass. Peak numbers match those described within the text and in Table 1. Color images available online at www.liebertonline.com/ast

$1567 \, cm^{-1}$ band is located at the Amide II absorption band position (Krimm and Bandekar, 1986). An absorption band at $1469 \, cm^{-1}$ relates to an asymmetric bending vibrational mode of aliphatic CH_3 or a CH_2 scissoring vibrational mode. The absorption band at $1434 \, cm^{-1}$ can be attributed to a C–O–H bending vibrational mode, and the band at $1401 \, cm^{-1}$ may represent the $N^+(CH_3)_3$ symmetric bending vibrational mode (Tamm and Tatulian, 1997).

Analyses directed at Spot 13 (Fig. 1c) are located within a glass shard that is crosscut by tubule bioalteration features (Fig. 4a, 4b). The clast also contains a zeolite-filled vug in the center and is surrounded by a palagonite rim.

Mineralogy. Mineralogical FTIR absorption bands are shown in Fig. 4c. The absorption band at $983 \, cm^{-1}$ is from the Si–O asymmetric stretching vibrational mode of SiO_4

tetrahedra, while that at $723 \, cm^{-1}$ could be a Si–O or Si–O–Al symmetric bending vibrational mode or a Ti–O stretching vibrational mode. An absorption band at $688 \, cm^{-1}$ represents the Ti–O stretching vibrational mode of TiO_6 octahedra. Bands at 3569, 3401, and $3270 \, cm^{-1}$ are assigned to the symmetric OH stretch of partially hydrogen-bonded water molecules, and asymmetric and symmetric OH stretch of water molecules that are fully hydrogen-bonded with surrounding water molecules, respectively (Verma *et al.,* 2007). This region is from the Si–OH stretching vibrations relating to the silicate mineral vibrations around $1000 \, cm^{-1}$, or from hydrogen bonded to the organic matrix.

Organics. Fourier transform infrared spectra were obtained from areas abundant with tubules (Fig. 4b) and are shown in Fig 4c. FTIR absorption bands of aliphatic CH
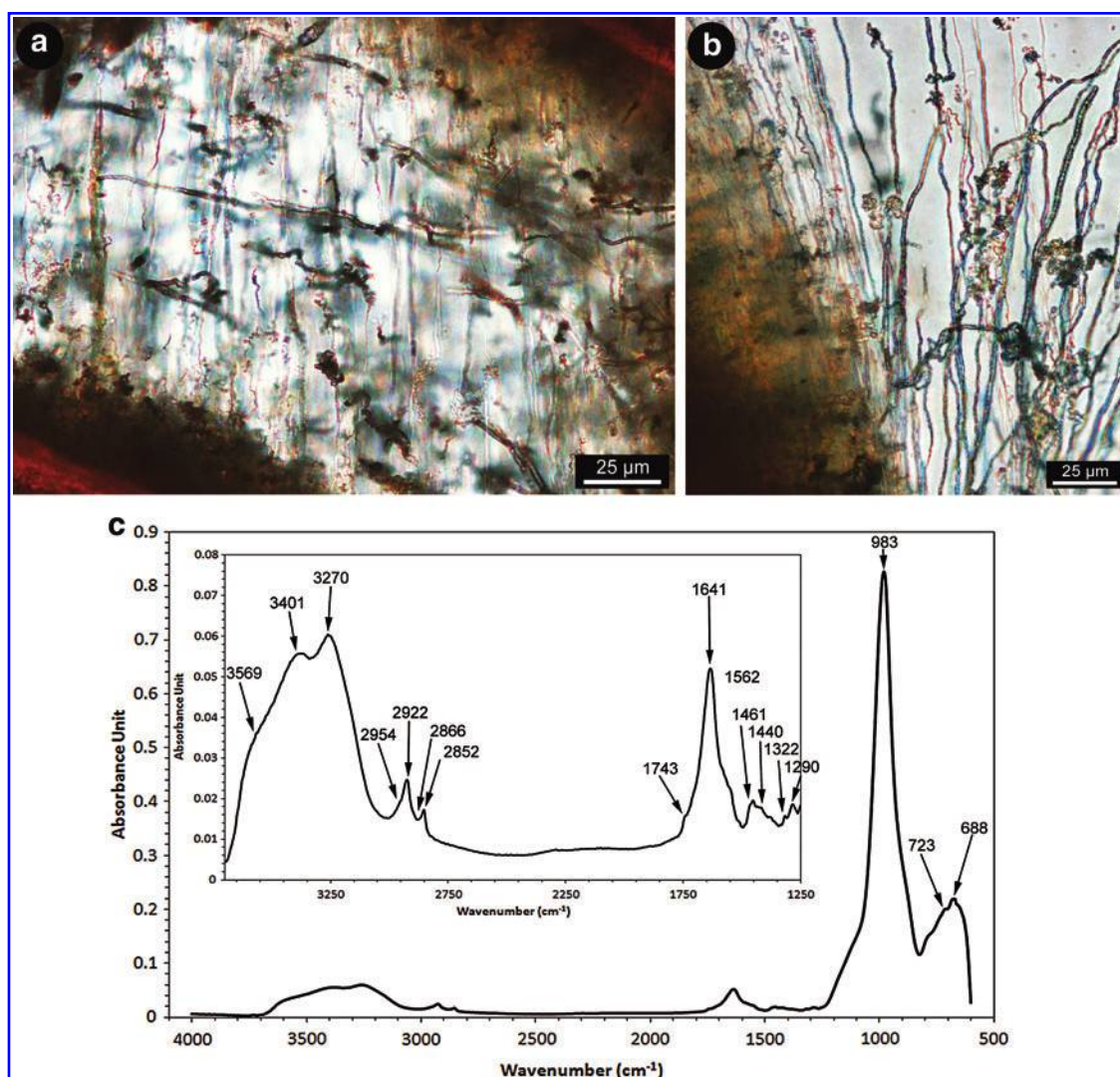
FIG. 4. Transmitted light images and FTIR absorbance spectra from Spot 13. (**a**) Transmitted light image of the edge of a glass clast where Spot 13 is taken. Both ichnofossil species identified previously are observed, with the larger *Tubulohyalichnus annularis* isp. nov. tubules visible crosscutting the clast and the smaller *Tubulohyalichnus simplus* isp. nov. extending out from the rims in dense clusters. (**b**) An extended depth of field image of a cluster of tubules at Spot 13. Loose tangles are observed near the ends of the tubules. (**c**) FTIR spectrum from Spot 13. Si–O and Ti–O stretching absorption bands are again observed with the main organic vibrational mode frequencies identified on the inset expanded absorbance spectrum. Peak numbers match those described within the text and in Table 1. Color images available online at www.liebertonline.com/ast

moieties appear at 2954, 2922, 2866, and 2852 cm^{-1}. The shoulder absorption bands at 2954 and at 2922 cm^{-1} are derived from the asymmetric stretching vibrational modes of aliphatic CH_3 and CH_2, respectively. The absorption bands at 2866 and 2852 cm^{-1} relate to the symmetric stretching vibrational modes of CH_3 and CH_2. There is an absorption band at 1743 cm^{-1} of the C=O stretch vibrational mode (Schmitt and Flemming, 1998). An absorption band at 1641 cm^{-1} may be derived from the Amide I C=O stretching vibrational mode. This same band, however, can be attributed to the H_2O bending vibrational mode. A shoulder at 1562 cm^{-1} can be assigned to an Amide II absorption band, and the absorption band at 1290 cm^{-1} that of an Amide III vibrational mode (Krimm and Bandekar, 1986). The absorption band at 1461 cm^{-1} is derived from an asymmetric bending vibrational mode of aliphatic CH_3. Absorption bands at 1440 and 1322 cm^{-1} are tentatively assigned to C–O–H bending and C–O stretching vibrational modes.

4.2. Tubule-free areas

The cores of glass clasts that were observed to contain no tubules (Figs. 5a and 6a) were also analyzed to allow com-parisons with the tubule-rich rims. Spot 9 and Spot 17 (Fig. 1c) are tubule-free cores of large irregular glass clasts (Figs. 5b and 6b).

An FTIR absorbance spectrum from the Spot 9 tubule-free core (Fig. 5c) indicates an absorption band located at 3401 cm^{-1} on a broad band centered at 3253 cm^{-1}. These are the asymmetric and symmetric OH stretching vibrational modes of water molecules that are fully hydrogen-bonded with surrounding water molecules (Verma *et al.*, 2007). The absorption band at 908 cm^{-1} is a Si–O asymmetric stretching vibrational mode of SiO_4 tetrahedra, and the 738 cm^{-1} absorption band is a Si–O or Si–O–Al symmetric bending, or a stretching vibrational mode of Ti–O (see Table 1). Both absorption bands are shifted to lower wavenumbers than those in the tubule-rich spectra.

Fourier transform infrared absorption spectra obtained from Spot 17 (Fig. 6c) contain a broad absorption band centered at 3274 cm^{-1} with a shoulder at 3407 cm^{-1} attributed to the symmetric and asymmetric OH stretching vibrational modes of water molecules that are fully hydrogen-bonded with surrounding water molecules. The absorption bands at 906 and 732 cm^{-1} are those of a Si–O asymmetric
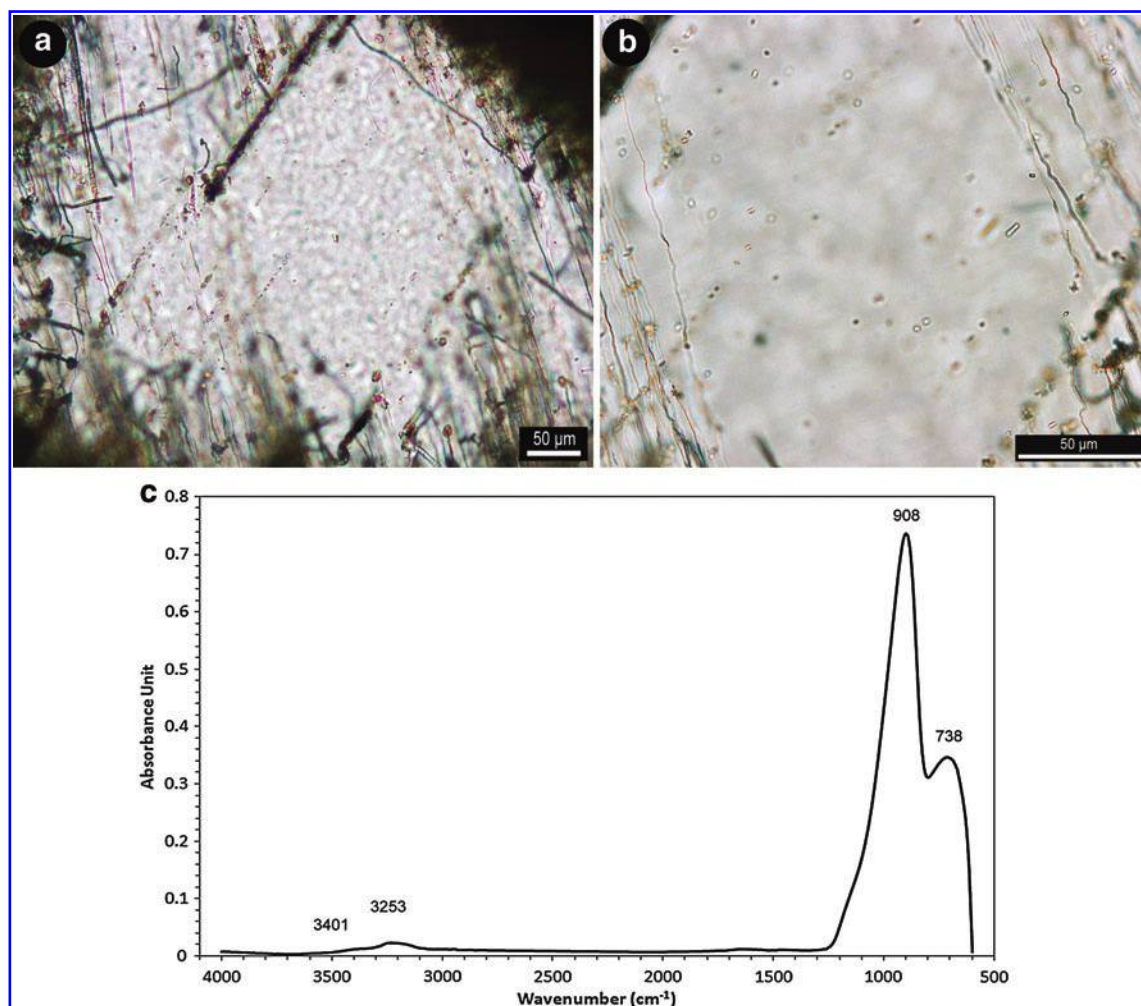
FIG. 5. Transmitted light images and FTIR absorbance spectrum from Spot 9. (**a**) Transmitted light image of a glass clast with a tubule-rich rim and tubule-free core. (**b**) Magnified view of the core of the glass clast, framed by *Tubulohyalichnus simplus* isp. nov., containing no evidence of tubules. (**c**) FTIR spectrum with Si–O and OH bands observed. No organic bands were observed. Color images available online at www.liebertonline.com/ast
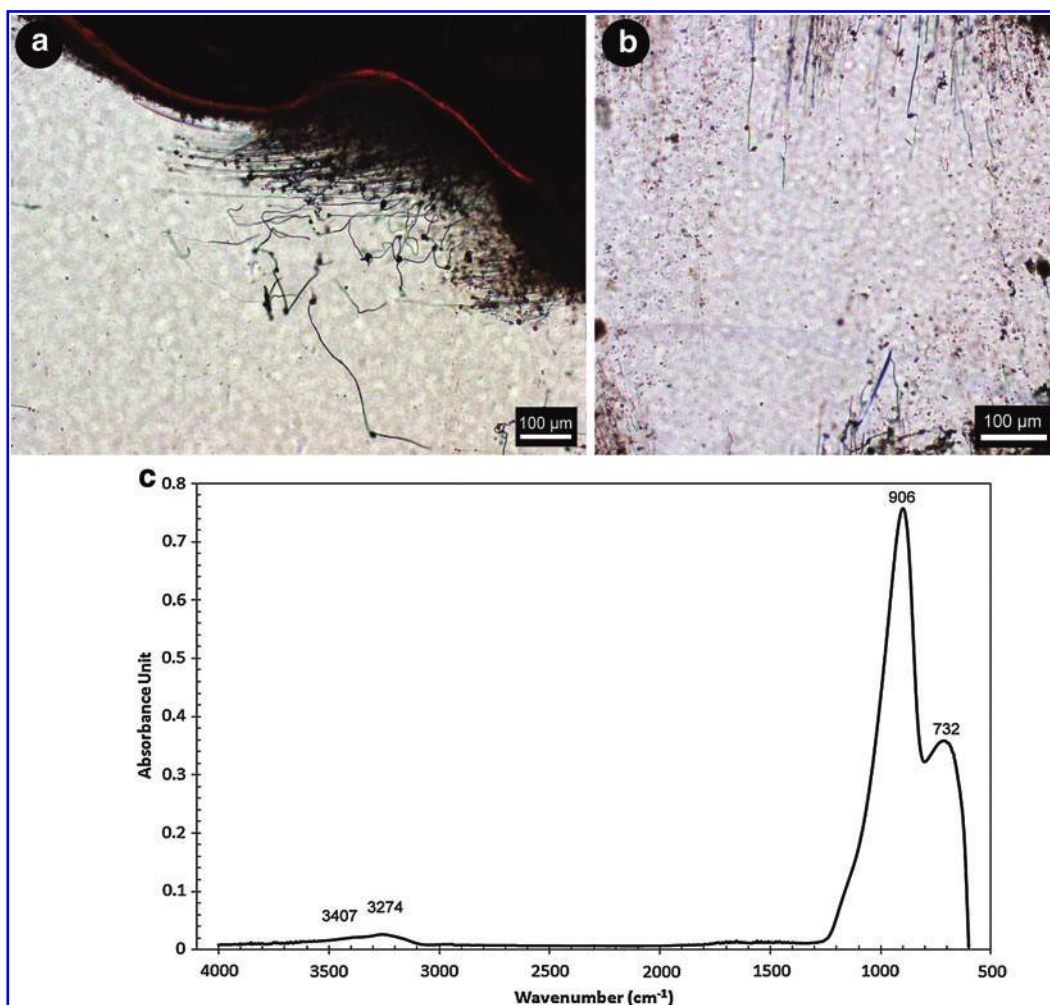
FIG. 6. Two transmitted light images and FTIR absorbance spectrum from Spot 17. (**a**) Overview image of the edge of a glass clast with a dense cluster of tubules radiating out from it. (**b**) Magnified view of the centre of the clast which lacks any visual evidence of tubules. (**c**) An FTIR spectrum with Si–O and OH band positions indicated. Color images available online at www.liebertonline.com/ast

stretching vibrational mode of SiO_4 tetrahedra and a symmetric bending vibrational mode of Si–O or Si–O–Al, or a Ti–O stretching vibrational mode (see Table 1).

5. Discussion and Interpretations

Infrared spectroscopy in the broadest sense has been applied to the study of microorganisms for nearly 60 years (*e.g.,* Heber *et al.,* 1952; Norris, 1959) based on the observation that different bacteria display different IR spectra. However, a bacterial cell or a biofilm represents an extremely complex system that creates many different signals from vibrations of molecules in the extracellular polymeric substances, the cell wall, the membrane, and the cytoplasm. The presence of these molecules within mineral matrices adds a further complicating factor in IR studies and determinations.

Analysis of the FTIR absorbance spectra obtained from this study indicates that the tubule-rich areas of glass clasts contain a number of organic absorption bands, which are lacking in the tubule-poor regions. The absorption bands that correspond to vibrational modes of Si–O and Ti–O corrobo-

rate previous data and observations regarding compositions of the glass clasts and accompanying minerals (*e.g.,* Banerjee and Muehlenbachs, 2003; Staudigel *et al.,* 2006; Benzerara *et al.,* 2007; Izawa *et al.,* 2010b). FTIR spectroscopy covering the region of 700–4000 cm^{-1} was therefore a highly appropriate tool for this study and enabled identification of both the minerals found in association with the glass clasts and the organics preserved within the tubule features.

5.1. Mineralogy

The major spectral features observed in most silicate minerals and silicate glasses are due to Si–O–Si, Si–O–Al and/or Al–O–Al fundamental vibrational modes (*e.g.,* McMillan, 1984; McMillan and Hofmeister, 1988). Asymmetric stretching vibrational modes contribute to about five bands relating to structural units in silicate glasses between 700 and 1250 cm^{-1} (*e.g.,* Bell *et al.,* 1968; Furukawa *et al.,* 1981; McMillan, 1984; Dowty, 1987; Poe *et al.,* 1992; Parot-Rajaona *et al.,* 1994; Agarwal *et al.,* 1995; McMillan and Wolf, 1995; McMillan *et al.,* 1998; King *et al.,* 2004; Dalby and King,

2006). Individual absorption bands are, however, difficult to discern in silicate glasses; instead a broad band can be seen centered at ~ 900–$1100\,cm^{-1}$, which shifts to higher wavenumbers as a function of increasing mol % SiO_2 (e.g., Heaton and Moore, 1957; Sweet and White, 1969).

In the Ontong Java glass sample, these broad absorption bands are centered on $980\,cm^{-1}$ in the tubule-rich areas and $910\,cm^{-1}$ in the tubule-free glass cores. The higher wavenumber absorption bands may be caused by a greater amount of SiO_2 in the tubule-rich areas than occurs in the glass cores that are essentially void of tubules. Benzerara et al. (2007) reported that the tubules are surrounded by an amorphous silica-rich rim, with palagonite composed of fine intergrowths of clays, oxides, and/or amorphous phases within the tubules. This indicates that the tubule-rich areas will have a higher SiO_2 content than the cores, which is reflected by a higher wavenumber band position for the SiO_2 vibrational modes. The network-forming cations Si and Al, as well as network-modifying cations, including Fe, Ti, Mg, Ca, Na, and K, have also been observed within the glasses with a variety of electron-beam, X-ray, and ion-beam techniques (e.g., Banerjee and Muehlenbachs, 2003; Benzerara et al., 2007; Banerjee et al., 2010). The presence of multiple network-forming and network-modifying cations may influence the wavenumber position of the Si–O absorption bands.

Regarding the tubule-rich areas, absorption bands appear between 680 and $690\,cm^{-1}$, and between 720 and $740\,cm^{-1}$. These are tentatively assigned to the Ti–O stretching vibrational modes of TiO_6 octahedra based on studies by Zhang et al. (2002). Titanium-rich minerals, such as titanite, are particularly important in the preservation of traces of microbial activity in basaltic glass (e.g., Furnes et al., 2004; Banerjee et al., 2006, 2007, 2008; Izawa et al., 2010b) in that they enable the preservation of morphological and/or chemical signatures of biological activity. Enrichments of titanium have been observed in association within tubules in the basaltic glass of this study and were previously documented by Banerjee and Muehlenbachs (2003). The Ti–O absorption bands of this study coincide with areas that were previously documented to contain titanite by using micro X-ray diffraction (Izawa et al., 2010b). The OH absorption bands observed around 3250 and $3400\,cm^{-1}$ are common to all spectra obtained, which indicates that the samples are hydrated. The water molecules are most likely bound to the glass within the samples. The absorption band at $\sim 3570\,cm^{-1}$ of the symmetric OH stretching vibrational mode of partially hydrogen-bonded water molecules can be identified in all spectra from the tubule-rich areas but is absent in those from the tubule-free cores. The water molecules may only be spectrally visible when bound to an organic matrix, so they are only observed in tubule-rich spectra. The H_2O absorption band commonly located at $\sim 1645\,cm^{-1}$ overlaps with that of the Amide I absorption band described later. An absorption band with a high absorbance is located at this wavenumber within the tubule-rich spectra but is very minor to absent in the glass core spectra.

5.2. Organics

This work has identified a number of distinct functional group frequencies belonging to aliphatic hydrocarbons, amides, and carboxylic acids, which may be assigned to various functional groups in lipids, proteins, and carboxylic acids (see Table 1 for the absorption bands identified and potential assignments). Although these groups can be found as part of the structure of other organic compounds, their spatial association with the tubular bioalteration patterns (e.g., Fisk et al., 1998; Furnes et al., 2001a), and the organic carbon and nucleic acids (Banerjee and Muehlenbachs, 2003; Benzerara et al., 2007) already detected within the structures, adds weight to the inference that these FTIR absorption bands likely reflect biomolecules produced by past microbial inhabitants of the tubules.

The aliphatic C–H stretching vibrational bands between 3000 and $2800\,cm^{-1}$ may be derived from groups usually present in fatty acid components of cell membranes (Helm et al., 1991). The symmetric and asymmetric CH_2 stretching vibrational modes in this region have higher absorbance values than the CH_3 absorption bands in the FTIR spectra. This indicates the highly aliphatic nature of the tubule areas under analysis and potentially the organisms that created the tubules. A predominance of methylene-chain CH_2 over end-methyl CH_3 has been used to indicate a dominant presence of long and straight aliphatic chains (i.e., fatty acids; Igisu et al., 2009). Within a single FTIR spectrum of this study, there were four CH_2 and four CH_3 vibrational modes detected, which indicates that neither aliphatic functional group is dominant in these samples. A comparison of the ratio of the asymmetric CH_2 and CH_3 stretching vibrational modes can be used to assess chain lengths and the degree of branching of the aliphatic structures present. A low CH_2/CH_3 band intensity ratio indicates a shorter, more branched aliphatic structure. Conversely, a higher ratio indicates a long and less-branched aliphatic chain (Lin and Ritz, 1993).

The expanded C–H stretching vibrational absorption bands for spot locations 4, 6, and 13 produced CH_2/CH_3 band intensity ratios of 4.9, 4.2, and 4.4, respectively. A CH_2/CH_3 ratio ≤ 2 signifies a biopolymer containing shorter and more branched aliphatic structures (Lin and Ritz, 1993; Marshall et al., 2005). The ratio values of this study are considered moderately high as described for Tasmanites by Lin and Ritz (1993), which implies that a biopolymer is present within the tubules consisting of aliphatic structures that are slightly longer and less branched. Considering the equal number of CH_2 and CH_3 absorption bands identified through FTIR analyses, these tubules may contain a mixture of branched and less-branched aliphatic structures. It was also proposed by Lin and Ritz (1993), and applied by Marshall et al. (2007), that the CH_2/CH_3 intensity ratio values can be correlated to the chain length of the aliphatic structures (i.e., the CH_2/CH_3 ratio should increase as the aliphatic chains become longer). The values in this study would therefore imply an n-alkane chain length of about 12 carbons; however, this is an oversimplified model and should be used in conjunction with other evidence.

The CH_2 and CH_3 ratios of spectra obtained from preserved microfossils are proposed to reflect the chemical composition of their precursor membrane lipids. Igisu et al. (2009) proposed a reversal of the CH_2/CH_3 ratio, called the $R_{3/2}$, whereby the peak heights of the absorbance bands of asymmetric CH_3 and asymmetric CH_2 are used. They proposed that a low $R_{3/2}$, between 0.3 and 0.5, is indicative of bacterial lipids. The intensity of the asymmetric CH_3 and

CH_2 absorbance bands of this study yield ratio values of 0.43, 0.47, and 0.67 for Spots 4, 6, and 13, which implies that bacterial lipids might be present within the tubules. $R_{3/2}$ values for fossilized coccoids and filaments observed within the Gunflint Formation are 0.45 ± 0.04 ($n=5$) for aggregated filaments and coccoids, and 0.43 ± 0.11 ($n=10$) for amorphous organic matter (Igisu *et al.*, 2009). These values match the majority of those in this study. The value of 0.67 obtained may signify an increase in branching of the aliphatic chains or indicate an archaeal component within the tubules. Studies by Igisu *et al.* (2009) also included $R_{3/2}$ analyses of extant bacteria and cell components as comparisons to their fossilized observations. A value of 0.65 was obtained through analysis of cyanobacteria whole cells. Some tubule structures of this study may therefore contain extant as well as fossilized bacteria, which would generate a range of $R_{3/2}$ values. Both aliphatic C–H ratio methods proposed indicate that the tubules of this study contain aliphatic hydrocarbons with both long and short carbon chains, with variable degrees of branching, which may be of bacterial lipid origins.

Most of the important vibrational modes associated with lipids (Tamm and Tatulian, 1997) were identified in the FTIR spectra from the tubule-rich areas of this study; for example, the absorption band at $1743 \, cm^{-1}$ is that of a $C=O$ stretching vibrational mode of esters found within fatty acids. All absorption bands are listed in Table 1. These functional groups are frequently encountered within membrane lipids, which may be an indication of the source for the organic functional groups found within the tubule-rich areas.

The IR spectra of polypeptides exhibit a number of amide absorption bands, which represent different vibrational modes of the peptide bond. An absorption band at $1637 \, cm^{-1}$ may be derived from the Amide I $C=O$ stretching vibrational mode (*e.g.*, Byler and Susi, 1986; Arrondo *et al.*, 1993; Goormaghtigh *et al.*, 1994; Jackson and Mantsch, 1995). If this vibrational mode is assumed to be a protein backbone vibration, then its wavenumber might indicate a β-sheet secondary structure. The Amide I band is most widely used for secondary structure analyses. Amide II absorption bands of secondary protein structures appear at $1567 \, cm^{-1}$ and at $1290 \, cm^{-1}$; an Amide III absorption band was identified in most spectra. These amide vibrational modes are additional evidence that organics, maybe of biological origin, are preserved within the tubule-rich areas. Previous studies of biomolecule preservation (Preston *et al.*, 2011) have indicated that, over geological time, the observation of amide absorption bands within rocks decreases, whereas aliphatic hydrocarbons are more persistent. This observation may imply that the tubules of this study are geologically young and/or that agents such as titanite are aiding long-term preservation of organics.

The Amide I absorption band overlaps with that of H_2O; however, both are expected to be present within the samples. The H_2O absorption band is mirrored by the existence of bands around $3300 \, cm^{-1}$, while the Amide I assignment is strengthened by the Amide II and Amide III absorption bands. Further deconvolution of these bands caused artifacts to be created in the spectra that hindered more detailed interpretations. An absorption band at $1700 \, cm^{-1}$ may be the stretching vibrational mode of a $C=O$ ester of a carboxylic group (Schmitt and Flemming, 1998), and the absorption bands below $1500 \, cm^{-1}$ are tentatively linked to vibrational modes of a number of carboxylic groups.

The organic absorption bands of this study correlate with those commonly found within membrane lipids and create spectra that resemble those obtained from biofilms (*e.g.*, Schmitt and Flemming, 1998). The identification of these organic bands within a single FTIR spectrum spatially associated with the tubules, and correlated to previous research that identified organic carbon and nucleic acids, may imply that the FTIR spectra are displaying molecular vibrations from biomolecules linked to the microorganisms that created the tubules.

6. Implications for Astrobiology

Meteorites, remote sensing spectroscopic investigations, and robotic exploration studies have shown us that basalts are among the most widespread rocks in the solar system. Therefore, basaltic glasses are expected to be widespread and can form anywhere basaltic melts are quenched. Basaltic glass can provide chemical energy and nutrients in the form of reduced Fe and Mn, as well as transition metals that are commonly found in cofactors and coenzymes (*e.g.*, Staudigel *et al.*, 2008a). Numerous lines of evidence indicate that, in the presence of liquid water, basaltic glass interacts in such a way as to create a habitat suitable for microbial colonization. Basaltic glass in contact with liquid water may therefore constitute a habitable environment during the early stages of solar system formation. The record of basaltic glass bioalteration on Earth extends to at least 3.5 Ga and has remained remarkably consistent through geological time (Furnes *et al.*, 2004; Banerjee *et al.*, 2006). The habitat provided by basaltic glass is a potential refuge from impact bombardment and irradiation. Basaltic glass may remain an important habitat on icy satellites such as Europa and Enceladus, in the deep subsurface of Mars, and in martian impact craters and post-impact hydrothermal systems (Izawa *et al.*, 2010a). Mars in particular is known to host abundant basaltic rock, and numerous lines of evidence indicate that liquid water has interacted with the crust, at least transiently, for much of Solar System history.

This study can also be applied to the investigation of life on early Earth. Previous studies into the biological affinities of Proterozoic microfossils to allow further elucidation into early life on Earth have been conducted (*e.g.*, Arouri *et al.*, 1999; Marshall *et al.*, 2005, 2007; Javaux and Marshall, 2006), and the preservation of organics within ancient rocks on Earth have been investigated with spectroscopy by Schopf *et al.* (2002), Schopf and Kudryavtsev (2005, 2009), Derenne *et al.* (2008), Lepot *et al.* (2008, 2009), Preston *et al.* (2008), Igisu *et al.* (2009), Preston and Genge (2010), and Preston *et al.* (2011). FTIR spectroscopic analyses have shown that aliphatic hydrocarbons and amides potentially related to fatty acids and proteins, respectively, can be detected within 396 Ma hydrothermal silica deposits (Preston and Genge, 2010). The combined evidence from previous studies of ancient preserved organics, combined with those preserved within basaltic glasses of this study, increases the possibility that organics from Archean-age rocks will be uncovered in the future through FTIR spectroscopic techniques to enable a further constraint on the date of the emergence of life on Earth.

The astrobiological implications of this study are amplified by the use of FTIR spectroscopy, which itself is a powerful tool for astrobiology. FTIR spectroscopy allows for nondestructive characterization of organic matter associated with microbial textures in rocks *in situ* with a high degree of chemical specificity. In reference to this study, the nondestructive aspect of FTIR spectroscopy is highly beneficial due to the critical nature of morphology in the interpretation of tubular and granular textures as biogenic features. Other methods for *in situ* analysis of carbon compounds cannot unambiguously identify organic carbon (EPMA, SEM-EDX); are destructive and fragment organic compounds, which complicates interpretation (ToF-SIMS); and can identify the presence of organic carbon but not its cellular host or hosts (STXM, TEM-EELS). Such methods can also contaminate the sample, and they are subject to interference from mineral phases. FTIR spectroscopy also provides advantages for the mitigation of contamination, a perennial difficulty in biomarker research. In contrast to whole-rock acid dissolution or combustion techniques, samples for *in situ* IR spectroscopy can be carefully treated to minimize contamination, as in the present study. We anticipate that spectromicroscopy techniques similar to those used in the present study will be profitably applied to highly contamination-sensitive samples, including martian meteorites and future sample returns.

7. Conclusions

Several independent lines of evidence support a biological origin for tubular features within volcanic glass shards. Organic carbon and nucleic acids associated with tubules have been previously identified; however, further details regarding the carbon species present have been elusive. This study adds FTIR spectroscopy to the previous suite of techniques employed to help further constrain the nature of these carbon compounds. We identified FTIR absorption bands that match those of aliphatic hydrocarbons, amides, esters, and carboxylic groups, which, along with the morphological evidence and results of previous investigations, may indicate an origin from fatty acids and proteins left over from previous biological inhabitants of the tubules. These may have been incorporated into, and preserved by, the titanite and/or palagonite precipitates within the tubules, or they may be biomolecules from the tubule-forming microorganisms that still exist within the glasses but, in time, may decay.

Acknowledgments

Author Disclosure Statement

Abbreviations

ATR, attenuated total reflectance; FTIR, Fourier transform infrared; ODP, Ocean Drilling Program; OJP, Ontong Java Plateau.

References

Agarwal, A., Davis, M., and Tomozawa, M. (1995) A simple IR spectroscopic method for determining fictive temperature of silica glasses. *J Non Cryst Solids* 185:191–198.

Arouri, K., Greenwood, P.F., and Walter, M.R. (1999) A possible chlorophycean affinity of some Neoproterozoic acritarchs. *Org Geochem* 30:1323–1337.

Arrondo, J.L.R., Muga, A., Castresana, J., and Goñi, F.M. (1993) Quantitative studies of the structure of proteins in solution by Fourier transform infrared spectroscopy. *Prog Biophys Mol Biol* 59:23–56.

Banerjee, N.R. and Muehlenbachs, K. (2003) Tuff life: bio-alteration in volcaniclastic rocks from the Ontong Java Plateau. *Geochemistry, Geophysics, Geosystems* 4, doi:10.1029/2002GC000470.

Banerjee, N.R., Honnorez, J., and Muehlenbachs, K. (2004) Low-temperature alteration of submarine basalts from the Ontong Java Plateau. In *Origin and Evolution of the Ontong Java Plateau,* Geological Society Special Publication 229, edited by J.G. Fitton, J.J. Mahoney, P.J. Wallace, and A.D. Saunders, Geological Society Publishing House, Bath, UK, pp 259–273.

Banerjee, N.R., Furnes, H., Muehlenbachs, K., Staudigel, H., and de Wit, M. (2006) Preservation of 3.4–3.5 Ga microbial bio-markers in pillow lavas and hyaloclastites from the Barberton Greenstone Belt, South Africa. *Earth Planet Sci Lett* 241:707–722.

Banerjee, N.R., Simonetti, A., Furnes, H., Muehlenbachs, K., Staudigel, H., Heaman, L., and Van Kranendonk, M.J. (2007) Direct dating of Archean microbial ichnofossils. *Geology* 35:487–490.

Banerjee, N.R., Furnes, H., Muehlenbachs, K., Staudigel, H., McLoughlin, N., and Bebout, G. (2008) Biogeochemical tracers of modern and ancient life in seafloor lavas. *Geochim Cosmochim Acta* 72:A51.

Banerjee, N.R., Izawa, M.R.M., Sapers, H.M., and Whitehouse, M.J. (2010) Geochemical biosignatures preserved in microbially altered basaltic glass. *Surf Interface Anal* 43:452–457.

Bell, R.J., Bird, N.F., and Dean, P. (1968) The vibrational spectra of vitreous silica, germania and beryllium fluoride. *Journal of Physics C: Solid State Physics* 1:299–303.

Benzerara, K., Menguy, N., Banerjee, N.R., Tyliszczak, T., Brown, G.E., Jr., and Guyot, F. (2007) Alteration of submarine basaltic glass from the Ontong Java Plateau: a STXM and TEM study. *Earth Planet Sci Lett* 260:187–200.

Blob, A.K., Rullkotter, J., and Welte, D.H. (1987) Direct determination of the aliphatic carbon content of individual macerals in petroleum source rocks by near infrared microspectroscopy. *Org Geochem* 13:1073–1077.

Brenner, D. (1984) Microscopic IR spectroscopy of coals. In *Chemistry and Characterization of Coal Macerals,* ACS Symposium Series 252, edited by R.E. Winans and J.C. Crelling, American Chemical Society, Washington DC, pp 47–64.

Byler, D.M. and Susi, H. (1986) Examination of the secondary structure of proteins by deconvolved FTIR spectra. *Biopolymers* 25:469–487.

Coffin, M.F. and Eldholm, O. (1993) Scratching the surface: estimating dimensions of large igneous provinces. *Geology* 21:515–518.

Dalby, K.N. and King, P.L. (2006) A new approach to determine and quantify structural units in silicate glasses using micro Fourier transform infrared spectroscopy. *Am Mineral* 91:1783–1793.

Derenne, S., Robert, F., Skrzypczak-Bonduelle, A., Gourier, D., Binet, L., and Rouzaud, J.-N. (2008) Molecular evidence for life in the 3.5 billion year old Warrawoona chert. *Earth Planet Sci Lett* 272:476–480.

Diem, M. (1993) *Introduction to Modern Vibrational Spectroscopy,* John Wiley & Sons, New York.

Dowty, E. (1987) Vibrational interactions of tetrahedra in silicate glasses and crystals: I. Calculations on ideal silicate-aluminate-germanate structural units. *Physics and Chemistry of Minerals* 14:80–93.

Dufresne, C.D.M., King, P.L., Dyar, M.D., and Dalby, K.N. (2009) Effect of SiO_2, total FeO, Fe^{3+}/Fe^{2+}, and alkali elements in basaltic glasses on mid-infrared spectra. *Am Mineral* 94:1580–1590.

Fisk, M.R., Giovannoni, S.J., and Thorseth, I.H. (1998) Alteration of oceanic volcanic glass: textural evidence of microbial activity. *Science* 281:978–980.

Furnes, H. and Muehlenbachs, K. (2003) Bioalteration recorded in ophiolitic pillow lavas. *Geological Society, London, Special Publications* 218:415–426.

Furnes, H., Staudigel, H., Thorseth, I.H., Torsvik, T., Muehlenbachs, K., and Tumyr, O. (2001a) Bioalteration of basaltic glass in the oceanic crust. *Geochemistry, Geophysics, Geosystems* 2, doi:10.1029/2000GC000150.

Furnes, H., Muehlenbachs, K., Torsvik, T., Thorseth, I.H., and Tumyr, O. (2001b) Microbial fractionation of carbon isotopes in altered basaltic glass from the Atlantic Ocean, Lau Basin, and Costa Rica Rift. *Chem Geol* 173:313–330.

Furnes, H., Banerjee, N.R., Muehlenbachs, K., Staudigel, H., and de Wit, M. (2004) Early life recorded in Archean Pillow Lavas. *Science* 304:578–581.

Furnes, H., McLoughlin, N., Muehlenbachs, K., Banerjee, N.R., Staudigel, H., Dilek, Y., de Wit, M., Van Kranendonk, M., and Schiffman, P. (2008) Oceanic pillow lavas and hyaloclastites as habitats for microbial life through time—a review. In *Links Between Geological Processes, Microbial Activities & Evolution of Life,* edited by Y. Dilek, H. Furnes, and K. Muehlenbachs, Springer, New York, pp 1–68.

Furukawa, T., Fox, K.E., and White, W.B. (1981) Raman spectroscopic investigation of the structure of silicate glasses. III. Raman intensities and structural units in sodium silicate glasses. *J Chem Phys* 75:3226–3237.

Goormaghtigh, E., Cabiaux, V., and Ruysschaert, J.-M. (1994) Determination of soluble and membrane protein structure by Fourier transform infrared spectroscopy. I. Assignments and model compounds. II. Experimental aspects, side chain structure, and H/D exchange. III. Secondary structures. In *Physicochemical Methods in the Study of Biomembranes,* Subcellular Biochemistry, Vol. 23, edited by H.J.

Hilderson and G.B. Ralston, Plenum Press, New York, pp 329–450.

Goos, F. and Hähnchen, H. (1964) Neumessung des Strahlenversatzeffektes bei Totalreflexion. *Ann Phys* 5:251–283.

Griffiths, P.R. and de Haseth, J.A., editors. (1986) *Fourier Transform Infrared Spectrometry,* Wiley, New York.

Günzler, H. and Gremlich, H.-U. (2002) *IR Spectroscopy: An Introduction,* Wiley-VCH, Weinheim.

Harrick, N.J. (1967) *Internal Reflection Spectroscopy,* John Wiley & Sons, New York.

Heaton, H.M. and Moore, H. (1957) A study of glasses consisting mainly of the oxides of elements of high atomic weight. Part II. The sources of the infrared absorption bands observed in the transmission curves of the glasses. *Journal of the Society of Glass Technology* 41:28–71.

Heber, J.R., Sevenson, R., and Boldman, O. (1952) Infrared spectroscopy as a means for identification of bacteria. *Science* 116:111–112.

Helm, D., Labischinski, H., Schallehn, G., and Naumann, D. (1991) Classification and identification of bacteria by Fourier-transform infrared spectroscopy. *J Gen Microbiol* 137:69–79.

Igisu, M., Ueno, Y., Shimojima, M., Nakashima, S., Awramik, S.M., Ohta, H., and Maruyama, S. (2009) Micro-FTIR spectroscopic signatures of bacterial lipids in Proterozoic microfossils. *Precambrian Res* 173:19–26.

Izawa, M.R.M., Banerjee, N.R., Flemming, R.L., Bridge, N.J., and Schultz, C. (2010a) Basaltic glass as a habitat for microbial life: implications for astrobiology and planetary exploration. *Planet Space Sci* 58:583–591.

Izawa, M.R.M., Banerjee, N.R., Flemming, R.L., and Bridge, N.J. (2010b) Preservation of microbial ichnofossils in basaltic glass by titanite mineralization. *Can Mineral* 48:1255–1265.

Jackson, M. and Mantsch, H.H. (1995) The use and misuse of FTIR spectroscopy in the determination of protein structure. *Crit Rev Biochem Mol Biol* 30:95–120.

Javaux, E.J. and Marshall, C.P. (2006) A new approach in deciphering early protist paleobiology and evolution: combined microscopy and microchemistry of single Proterozoic acritarchs. *Rev Palaeobot Palynol* 139:1–15.

King, P.L., McMillan, P.F., and Moore, G.M. (2004) Infrared spectroscopy of silicate glasses with application to natural systems. In *Infrared Spectroscopy in Geochemistry, Exploration Geochemistry and Remote Sensing,* Short Course Series 33, edited by P. King, M. Ramsey, and G. Swayze, Mineralogical Association of Canada, Québec, pp 93–133.

Krimm, S. and Bandekar, J. (1986) Vibrational spectroscopy and conformation of peptides, polypeptides, and proteins. *Adv Protein Chem* 38:181–364.

Landais, P. and Rochdi, A. (1990) Reliability of semi-quantitative data extracted from transmission microscopy–Fourier transform infrared spectra of coal. *Energy Fuels* 4:290–295.

Lepot, K., Benzerara, K., Brown, G.E., and Philippot, P. (2008) Microbially influenced formation of 2724-million-year-old stromatolites. *Nat Geosci* 1:118–121.

Lepot, K., Philippot, P., Benzerara, K., and Wang, G.-Y. (2009) Garnet-filled trails associated with carbonaceous matter mimicking microbial filaments in Archean basalt. *Geobiology* 7:393–402.

Levenberg, K.Q. (1944) A method for the solution of certain problems in least squares. *Quarterly of Applied Mathematics* 2:164–168.

Lin, R. and Ritz, G.P. (1993) Reflectance FT-IR microspectroscopy of fossil algae contained in organic-rich shales. *Appl Spectrosc* 47:265–271.

Mahoney, J.J. (1987) An isotopic survey of Pacific oceanic plateaus: implications for their nature and origin. In *Seamounts, Islands, and Atolls,* AGU Geophysical Monograph Series 43, edited by B.H. Keating, P. Fryer, R. Batiza, and G.W. Boehlert, American Geophysical Union, Washington DC, pp 207–220.

Mahoney, J.J., Fitton, J.G., Wallace, P.J., *et al.* (2001) *Proceedings of the Ocean Drilling Program, Initial Reports* [online], Vol. 192, Ocean Drilling Program, College Station, TX. Available online at http://www-odp.tamu.edu/publications/192_IR/192ir.htm.

Marquardt, D.W. (1963) An algorithm for least-squares estimation of nonlinear parameters. *Journal of the Society for Industrial and Applied Mathematics* 11:431–441.

Marshall, C.P., Javaux, E.J., Knoll, A.H., and Walter, M.R. (2005) Combined micro-Fourier transform infrared (FTIR) spectroscopy and micro-Raman spectroscopy of Proterozoic acritarchs: a new approach to palaeobiology. *Precambrian Res* 138:208–224.

Marshall, C.P., Love G.D., Snape, C.E., Hill, A.C., Allwood, A.C., Walter, M.R., Van Kranendonk, M.J., Bowden, S.A., Sylva, S.P., and Summons, R.E. (2007) Structural characterization of kerogen in 3.4 Ga Archaean cherts from the Pilbara Craton, Western Australia. *Precambrian Res* 155:1–23.

McLoughlin, N., Furnes, H., Banerjee, N.R., Muehlenbachs, K., and Staudigel, H. (2009) Ichnotaxonomy of microbial trace fossils in volcanic glass. *J Geol Soc London* 166:159–169.

McMillan, P. (1984) Structural studies of silicate glasses and melts—applications and limitations of Raman spectroscopy. *Am Mineral* 69:622–644.

McMillan, P. and Wolf, G. (1995) Vibrational spectroscopy of silicate liquids. In *Structure, Dynamics and Properties of Silicate Melts,* Reviews in Mineralogy, Vol. 32, edited by J. Stebbins, P. McMillan, and D. Dingwell, Mineralogical Society of America, Chantilly, VA, pp 247–315.

McMillan, P.F. and Hofmeister, A.M. (1988) Infrared and Raman spectroscopy. In *Spectroscopy Methods in Mineralogy and Geology,* Reviews in Mineralogy, Vol. 18, edited by F.C. Hawthorne, Mineralogical Society of America, Chantilly, VA, pp 99–159.

McMillan, P.F., Grzechnik, A., and Chotalla, H. (1998) Structural characterization of SiO_2-$CsAlO_2$ and SiO_2-$RbAlO_2$ glasses. *J Non Cryst Solids* 226:239–248.

Norris, K.P. (1959) Infra-red spectroscopy and its application to microbiology. *J Hygiene* 57:326–345.

Painter, P.C., Snyder, R.W., Starsinic, M., Coleman, M.M., Kuehn, D.W., and Davis, A. (1981) Concerning the application of FT-infrared to the study of coal: a critical assessment of band assignments and the application of spectral analysis programs. *Appl Spectrosc* 35:475–485.

Parot-Rajaona, T., Coté, B., Bessada, C., Massiot, D., and Gervais, F. (1994) An attempt to reconcile interpretations of atomic vibrations and[29] Si NMR data in glasses. *J Non Cryst Solids* 169:1–14.

Peckmann, J., Bach, W., Behrens, K., and Reitner, J. (2008) Putative cryptoendolithic life in Devonian pillow basalt, Rheinisches Schiefergebirge, Germany. *Geobiology* 6:125–135.

Poe, B.T., McMillan, P.F., Angell, C.A., and Sato, R.K. (1992) Al and Si coordination in SiO_2-Al_2O_3 glasses and liquids: a study by NMR and IR spectroscopy and MD simulations. *Chem Geol* 96:333–349.

Preston, L.J. and Genge, M.J. (2010) The Rhynie Chert, Scotland and the search for life on Mars. *Astrobiology* 10:549–560.

Preston, L.J., Benedix, G., Genge, M.J., and Sephton, M.A. (2008) A combined mineralogical, textural and mid-infrared spectroscopy study of silica sinter deposits: applications to silica identification on Mars. *Icarus* 198:331–350.

Preston, L.J., Shuster, J., Fernández-Remolar, D., Banerjee, N.R., Osinski, G.R., and Southam, G. (2011) The preservation and degradation of filamentous bacteria and biomolecules in iron oxide deposits from Rio Tinto, Spain. *Geobiology* 9:233–249.

Rochdi, A. and Landais, P. (1991) Transmission micro-infrared spectroscopy: an efficient tool for microscale characterization of coal. *Fuel* 70:367–371.

Schmitt, J. and Flemming, H.-C. (1998) FTIR spectroscopy in microbial and material analysis. *International Biodeterioration & Biodegradation* 41:1–11.

Schopf, J.W. and Kudryavtsev, A.B. (2005) Three-dimensional Raman imagery of Precambrian microscopic organisms. *Geobiology* 3:1–12.

Schopf, J.W. and Kudryavtsev, A.B. (2009) Confocal laser scanning microscopy and Raman imagery of ancient microscopic fossils. *Precambrian Res* 173:39–49.

Schopf, J.W., Kudryavtsev, A.B., Agresti, D.G., Wdowiak, T.J., and Czaja, A.D. (2002) Laser-Raman imagery of Earth's earliest fossils. *Nature* 416:73–76.

Staudigel, H., Furnes, H., Banerjee, N.R., Dilek, Y., and Muehlenbachs, K. (2006) Microbes and volcanoes: a tale from the oceans, ophiolites, and greenstone belts. *GSA Today* 16:4–10.

Staudigel, H., Furnes, H., McLoughlin, N., Banerjee, N.R., Connell, L.B., and Templeton, A. (2008a) 3.5 billion years of glass bioalteration: volcanic rocks as a basis for microbial life? *Earth-Science Reviews* 89:156–176.

Staudigel, H., Furnes, H., McLoughlin, N., Banerjee, N.R., Connell, L.B., and Templeton, A. (2008b) Microbial glass bioalteration: inferring mechanisms of biocorrosion from trace fossil morphology. *Geochim Cosmochim Acta* 72:A893.

Stuart, B. (2004) *Infrared Spectroscopy: Fundamentals and Applications*, John Wiley & Sons, New York, pp 137–163.

Stuart, B.H. and Ando, D.J. (1997) *Biological Applications of Infrared Spectroscopy,* edited by B.H. Stuart and D.J. Ando, John Wiley & Sons, New York.

Sweet, J.R. and White, W.B. (1969) Study of sodium silicate glasses and liquids by infrared reflectance spectroscopy. *Physics and Chemistry of Glasses* 10:246–251.

Tamm, L.K. and Tatulian, S.A. (1997) Infrared spectroscopy of proteins and peptides in lipid bilayers. *Q Rev Biophys* 30:365–429.

Thiessen, R. (1925) Origin of the boghead coals. Geological Survey Professional Paper 132-I, U.S. Geological Survey, Reston, VA.

Thorseth, I.H., Furnes, H., and Heldal, M. (1992) The importance of microbiological activity in the alteration of natural basaltic glass. *Geochim Cosmochim Acta* 56:845–850.

Thorseth, I.H., Torsvik, T., Furnes, H., and Muehlenbachs, K. (1995) Microbes play an important role in the alteration of oceanic crust. *Chem Geol* 126:137–146.

Thorseth, I.H., Pedersen, R.B., and Christie, D.M. (2003) Microbial alteration of 0–30 Ma seafloor and sub-seafloor basaltic glasses from the Australian Antarctic discordance. *Earth Planet Sci Lett* 215:237–247.

Torsvik, T., Furnes, H., Muehlenbachs, K., Thorseth, I.H., and Tumyr, O. (1998) Evidence for microbial activity at the glass-alteration interface in oceanic basalts. *Earth Planet Sci Lett* 162:165–176.

Verma, D., Katti, K., and Katti, D. (2007) Nature of water in nacre: a 2D Fourier transform infrared spectroscopic study. *Spectrochim Acta A Mol Biomol Spectrosc* 67:784–788.

Zhang, M., Salje, E.K.H., Bismayer, U., Groat, L.A., and Malcherek, T. (2002) Metamictization and recrystallization of titanite: an infrared spectroscopic study. *Am Mineral* 87:882–890.

Address correspondence to:
Dr. Louisa Preston
Centre for Planetary Science and Exploration (CPSX)
Department of Earth Sciences
University of Western Ontario
1151 Richmond Street
London, Ontario
Canada
N6A 5B7

E-mail: lpresto5@uwo.ca

This article has been cited by:

1. Charles S. Cockell , Sherry L. Cady , Nicola McLoughlin . 2011. Introduction: Volcanism and Astrobiology: Life on Earth and Beyond. *Astrobiology* **11**:7, 583-584. [Citation] [Full Text] [PDF] [PDF Plus]